Biomaterials Science

ROYAL SOCIETY OF CHEMISTRY

REVIEW

View Article Online
View Journal

Cite this: DOI: 10.1039/d5bm01825k

Engineering delivery platforms for controlled nitric oxide release

Sang-Hun Choi, Chae Yeon Han, Kyeong Jin Cho, Kangmin No and Jihoon Kim *

Nitric oxide (NO) is a versatile gaseous signaling molecule with broad therapeutic potential in cardiovascular regulation, immune modulation, oncology, antibiotics, and tissue regeneration. However, its clinical application is severely constrained by physicochemical limitations, including poor aqueous solubility, rapid degradation, and the lack of spatiotemporal control over its release. To address these challenges, a diverse array of NO donors, ranging from spontaneous-release compounds to stimuli-responsive prodrugs, has been developed, each with distinct advantages and limitations. In this review, we classify representative NO donors into two major categories: unstable donors (*e.g.*, *N*-diazeniumdiolates, *S*-nitrosothiols, SIN-1) and stable donors (*e.g.*, O^2-protected diazeniumdiolates, protected SIN-1, nitrobenzene derivatives, BNN6). Here, we highlight recent advances in the engineering of delivery platforms, including polymeric nanoparticles, hydrogels, xerogels, liposomes, and various inorganic materials, which enable precise, stimuli-triggered NO release, improved stability, and tissue-specific targeting. By integrating NO donor chemistry with materials design, these platforms offer strong potential for controlled NO-based therapies across a wide range of biomedical applications. We conclude by outlining future directions and key challenges in translating NO delivery systems into clinically viable therapeutics.

Received 14th December 2025,
Accepted 12th January 2026

DOI: 10.1039/d5bm01825k

rsc.li/biomaterials-science

1. Introduction

Nitric oxide (NO) is an essential endogenous signaling molecule that plays key roles in vasodilation, neurotransmission, and immune regulation in the cardiovascular, nervous, and immune systems.[1–5] Motivated by its broad biological activity and therapeutic potential, extensive efforts over the past several decades have focused on developing NO-based therapeutics. Growing evidence supporting the effectiveness of NO in various disease settings, including angina, pulmonary hypertension, accelerated wound healing, infection control, and cancer therapy, has established NO as a promising next-generation biological therapeutic agent.[6–10] Nevertheless, the direct use of NO as a pharmaceutical agent remains highly challenging. First, as a gaseous molecule, NO has extremely low aqueous solubility and is rapidly oxidized in the bloodstream to form stable metabolites, making direct administration impractical.[11–15] Second, NO has an exceptionally short biological half-life and is cleared within seconds under physiological conditions, which increases the likelihood of inactivation before it reaches target tissues.[5,11,12,16] Third, achieving precise spatiotemporal control over NO delivery remains challenging, thereby increasing the risk of undesired systemic side effects and toxicity.[16–18] Collectively, these limitations severely limit the clinical translation of NO-based therapies.

Over the past several decades, researchers have introduced the concept of NO donors to address these challenges. NO donors are small molecules or macromolecular compounds that release NO in biological environments; early examples include simple organic nitrates.[8,19–21] Over time, more advanced NO donors such as *N*-diazeniumdiolates, *S*-nitrosothiols, and sydnonimines were developed, further expanding the scope of NO-based therapeutic applications.[8,22,23] However, these early donor systems shared a major limitation: poor control over the location and timing of NO release. Unstable NO donors, which release NO spontaneously, degrade at unpredictable rates under physiological conditions and often produce an initial burst of NO that can cause unintended cytotoxicity and disrupt normal physiological balance.[8,24,25] In contrast, stable NO donors were later designed to improve storage stability and allow stimuli-responsive release, but they frequently suffer from complex synthesis and limited bioavailability.[26]

In the past 10–15 years, significant progress has been made in the development of delivery platform-based NO release strategies to address these limitations. By incorporating NO donors into delivery platforms such as polymeric nanoparticles, hydrogels, liposomes, micelles, 2D nanomaterials, and metal–organic frameworks (MOFs), researchers have achieved more precise spatiotemporal control of NO release while simul-

School of Integrative Engineering, Chung-Ang University, Seoul 06974, South Korea.
E-mail: jihoonkim@cau.ac.kr; Tel: +82-2-820-5489

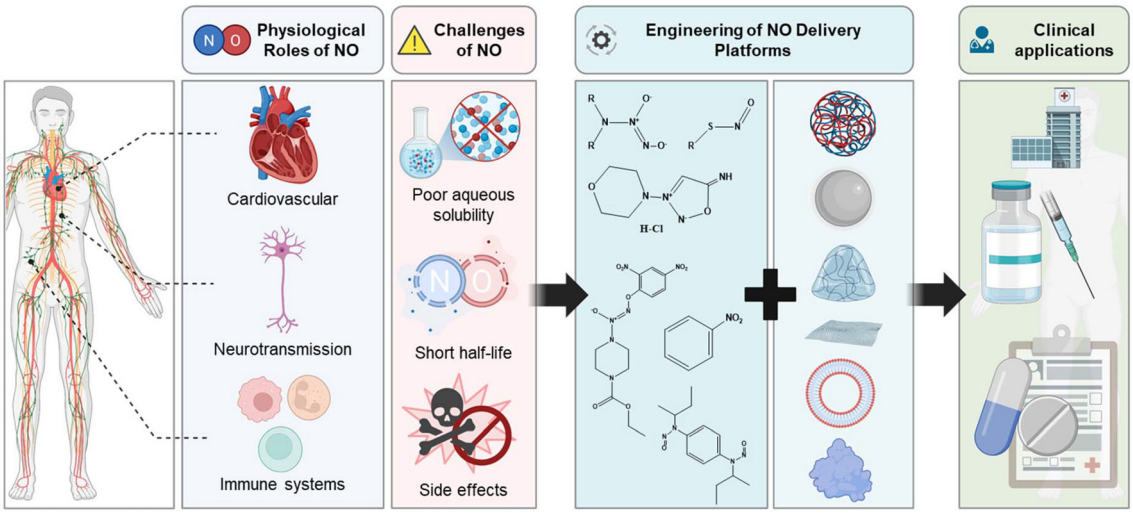

Fig. 1 Schematic illustration of the conceptual framework of this review. The figure presents the physiological roles and biological significance of NO, highlights the major challenges constraining its clinical application, illustrates the engineering strategies and diverse delivery platforms developed to overcome these limitations, and emphasizes the potential for advancing NO-based therapeutics toward clinical translation.

taneously enhancing storage stability. Importantly, these advances represent more than incremental gains in NO delivery efficiency; rather, they fundamentally broaden the clinical applicability of NO-based therapeutics.

In this review, we systematically examine the structural features, limitations, and delivery strategies of the various NO donors developed to date. Section 2 focuses on spontaneous-release ("unstable") NO donors, including *N*-diazeniumdiolates, *S*-nitrosothiols, and SIN-1, while section 3 covers stimuli-responsive ("stable") NO donors, including O^2-protected diazeniumdiolates, protected SIN-1, nitrobenzene derivatives, and BNN6. For each category, we discuss their biochemical properties, key limitations, and formulation strategies based on polymers, nanoparticles, photoreactive materials, and related technologies that have been developed to address these challenges (Fig. 1). Through this review, we aim to highlight the central role of delivery platform engineering in advancing NO-based therapeutics and to outline future directions in this rapidly developing field. Representative examples of engineered NO delivery platforms with varied donors, materials, and activation mechanisms are presented in Table 1. Importantly, the NO release kinetics discussed

Sang-Hun Choi

Sang-Hun Choi is a PhD candidate in the School of Integrative Engineering at Chung-Ang University. His research focuses on immunology-driven biomaterials, with a particular interest in the roles of nitric oxide (NO) and immune modulation in inflammatory diseases, including colitis. During his graduate training, he has developed interdisciplinary expertise at the interface of biomaterials, immunology, and disease modeling.

Jihoon Kim

Jihoon Kim is a tenure-track Assistant Professor in the School of Integrative Engineering at Chung-Ang University. Prior to his current appointment, he served as a tenure-track Assistant Professor at Yonsei University, Mirae Campus, for 1.5 years, a Research Scientist II at the Georgia Institute of Technology for one year, and a postdoctoral researcher at the Georgia Institute of Technology for five years, the National Institutes of Health for two years, and the Institute for Basic Science for one year. He received dual B.S. degrees in Life Science and Chemistry and earned his Ph.D. in Chemistry from Pohang University of Science and Technology (POSTECH). His research focuses on engineering delivery platforms for biologically reactive gases, small-molecule therapeutics, nucleotides, proteins, and peptides to advance therapeutic immunoengineering.

Table 1 Representative examples of engineered NO delivery platforms with varied donors, materials, and activation mechanisms

NO donor	Delivery platform	Material composition	Stimulus-triggered conditions	NO release profile and therapeutic efficacy	Therapeutic strategy	Ref.
N-Diazeniumdiolate (PEI-NONOate)	PLGA nanoparticles	Polyethylenimine (PEI) + poly (lactic-*co*-glycolic acid) (PLGA)	pH 7.4 (acid-catalyzed)	6-day sustained release, no initial burst; enhanced endothelial cell adhesion, proliferation, and angiogenesis	Monotherapy (NO only)	31
N-Diazeniumdiolate (SPER/NO, DPTA/NO)	Liposomes	DPPC + cholesterol (1 : 1 ratio), ~265 nm	pH 7.4 (blood) *vs.* pH 5.4 (tumor microenvironment)	4–7 fold prolonged half-life at pH 7.4; tumor-selective burst release; suppressed PANC-1 cell viability	Monotherapy (NO only)	41
N-Diazeniumdiolate (diazeniumdiolate-functionalized alkoxysilanes)	Sol–gel xerogel	Diazeniumdiolate-alkoxysilanes + phenyltrimethoxysilane (PTMOS) in silica matrix	37 °C, pH 7.4 (physiological)	High loading (1.2 μmol mg^{-1}); 20–90 hours sustained release; maintained glucose sensor sensitivity (3.4 nA mM^{-1}) for >7 days	Monotherapy (NO only)	42
S-Nitrosothiol (GSNO)	F127-*g*-gelatin hydrogel	Pluronic F127 conjugated with gelatin	37 °C; MMP-9 enzymatic degradation (tumor microenvironment)	Sustained NO release; synergistic antitumor effects with anti-CTLA-4 antibody-mediated T cell activation	NO + ICB (aCTLA-4 mAb)	57
S-Nitrosothiol (GSNO)	PLA microparticles in chitosan hydrogel	PLA microparticles (~40.7 μm, 45.6% encapsulation efficiency) in chitosan/β-glycerophosphate hydrogel	37 °C, pH 7.4 (physiological)	2-Fold extended duration; steady release (24–68 nM mg^{-1}) over 7 days; >85% HDF viability; hemolysis <5%	Monotherapy (NO only)	58
S-Nitrosothiol (SNAP, GSNO)	3D-printed RSNO-silicone	Silicone polymer (momentive) with PDMS coating (10 wt%); RSNO crystals (10–50 μm)	37 °C, pH 7.4 (gradual crystal dissolution)	4–7 fold prolonged (~29 days); 21% burst reduction; 66% reduced proteus mirabilis biofilm *vs.* control; 92% *vs.* commercial catheters	Monotherapy (NO only)	59
S-Nitrosothiol (SNAP)	Polymer–metal composite (PMC)	CarboSil polymer with metal nanoparticles (Cu, Fe, Ni, Zn, Ag); layered/non-layered	pH 7.4, 37 °C (metal-catalyzed decomposition)	Layered: moderated and prolonged release; Cu-based: highest MRSA reduction (~2.13 log); enhanced biocompatibility	Monotherapy (NO only)	60
S-Nitrosothiol (CysNO)	Upconversion-ZIF-8 (UCZN) nanocomposite	Upconversion nanoparticles (UCNPs) + ZIF-8 shell; ~10.6 nm	980 nm NIR laser → UV emission → S-NO bond cleavage	Excellent storage stability; rapid, reversible on–off NO burst; significant motor function recovery in spinal cord injury model	Monotherapy (NO only)	61
Sydnonimine (*N*-nitroso-SIN-1)	Protected SIN-1 derivative	SIN-1 with *N*-nitrosation modification	37 °C, pH 7.4 (physiological)	Up to 2 equivalents NO per molecule; reduced peroxynitrite generation; enhanced NO release efficiency; mitigated ROS production	Monotherapy (NO only)	75
Sydnonimine (SA-2: SIN-1 + nitroxide antioxidant)	PLGA nanoparticles	SIN-1 motif + nitroxide antioxidant in PLGA	37 °C, pH 7.4 (physiological)	Enhanced angiogenic activity at lower concentrations *vs.* free SIN-1; prolonged NO release; improved storage stability	Monotherapy (NO only)	76
O^2-protected diazeniumdiolate (JS-K)	pH/GSH-dual responsive Nanoparticles	Polymeric nanoparticle core with pH-sensitive shell; ~100–200 nm	pH 7.4 (inactive) *vs.* pH 6.5 (tumor); GSH 20 μM (inactive) *vs.* 10 mM (cytosol, active)	Burst-type NO release at dual triggers; enhanced Type I PDT effects; depleted intracellular GSH; significantly improved antitumor efficacy	NO + PDT (type I)	86
O^2-protected diazeniumdiolate (double JS-K)	PS-*b*-PEG or PLA-*b*-PEG nanoparticles	Polystyrene-PEG or PLA-PEG block copolymers; hydrophobic core	pH 7.4 (PBS); GSH 4 mM (physiological)	Ninefold increase in half-life (4.5 min free *vs.* 40 min encapsulated); substantially prolonged GSH-triggered activation	Monotherapy (NO only)	87
O^2-protected diazeniumdiolate (JS-K)	Pluronic P123 micelles	Pluronic P123 polymer; amphiphilic structure	Serum, blood, plasma, cell culture media (GSH-triggered)	Increased cellular uptake; greater cytoplasm and organelle accumulation *vs.* free JS-K	Monotherapy (NO only)	88

Table 1 *(Contd.)*

NO donor	Delivery platform	Material composition	Stimulus-triggered conditions	NO release profile and therapeutic efficacy	Therapeutic strategy	Ref.
O^2-protected diazeniumdiolate (JS-K)	P123/JS-K pluronic micelles	Pluronic P123 polymer	PBS, whole blood, plasma, cell culture (GSH-responsive)	Significantly greater stability; slower degradation; substantially greater tumor regression in HL-60 xenograft mouse model	Monotherapy (NO only)	84
O^2-protected diazeniumdiolate (P-NO)	POEGMA-*b*-PPBA polymeric micelles	Phenylboronic acid (PBA)-containing polymer + P-NO (diol moieties form boronate ester); core–shell	pH 7.4 (cytosol, active) *vs.* 5.0 (endolysosome, inactive); GSH 2 mM (active) *vs.* 50 μM (inactive)	Excellent blood stability; minimal NO leakage in circulation; cytosol-selective burst release; potent antitumor effects	Monotherapy (NO only)	89
Sydnonimine (SIN-1 glycosidase conjugates)	Glycosidase-activated prodrugs	Carbohydrate-linked SIN-1 *via* glycosyl carbamate (glucose, galactose, *N*-acetylneuraminic acid)	β-Glucosidase (240-fold enhancement); β-galactosidase (9.3-fold enhancement)	Excellent stability without enzyme; enzyme-specific NO release activation	Monotherapy (NO only)	90
Sydnonimine (SISIN-1, AL-SISIN-1)	Self-immolative prodrug (with BSA conjugate)	2,2′-Dithiodipyridine (PDS) + SIN-1; AL-SISIN-1: SISIN-1-BSA (~10.6 nm)	GSH 20 μM (extracellular, stable) *vs.* 2 mM (intracellular, active); lymph node uptake *via* SPARC/gp60	Highly stable extracellularly; rapid selective intracellular release; low systemic toxicity; significant lymph node metastatic cancer efficacy	Monotherapy (NO only)	91
Nitrobenzene (NTA: 4-nitro-3-(trifluoromethyl)aniline)	Lipid nanovesicles (Ves-NTA)	DPPC + amphiphilic NTA; 100–150 nm vesicles	410 nm blue light (reversible on/off)	Reversible on/off light control; half-life 22.0–38.5 min; higher Neuro-2A cell viability; tunable NO output	Monotherapy (NO only)	97
Nitrobenzene (Rol-DNB-mor/pyr)	Mitochondrial-targeted delivery	Nitrobenzene + mitochondrial targeting signal	530–590 nm visible light (*e.g.*, 562 nm, tissue-penetrating)	Mitochondrial-specific NO generation; selective regulation of mitochondrial fission; reduced phototoxicity	Monotherapy (NO only)	98
BNN6	pDA-coated Fe_3O_4 magnetic nanoparticles	Iron oxide (Fe_3O_4) core with polydopamine (pDA) shell; BNN6 loading	808 nm NIR light (photothermal); magnetic field targeting	Tunable NO release under NIR on/off control; magnetic targeting; potent antibacterial and biofilm-disrupting activity	Monotherapy (NO only)	106
BNN6	Bismuth titanate ($BiTiS_3$) nanosheet hybrid	Two-dimensional $BiTiS_3$ nanosheets + BNN6	808 nm NIR (photothermal + photoelectronic conversion)	Rapid, high-yield NO release; faster liberation than GO-BNN6; robust antitumor efficacy with combined photothermal therapy	NO + PTT ($BiTiS_3$ photothermal agent)	107
BNN6	Metal–organic frameworks (MOFs)	BNN6 encapsulated in MOF nanoplatforms (with photothermal agents)	808 nm NIR light	NIR-triggered combination therapies; integrated photothermal + NO therapy	NO + PTT (MOF-integrated photothermal agent)	108
BNN6	TRPV1-signaling nanocarriers	BNN6 in TRPV1-specific nanocarriers	Light-triggered (wavelength dependent on carrier design)	Light-controllable gaseous signaling in neurological disease models; precise spatiotemporal NO control	Monotherapy (NO only)	109
BNN6	3D hydrogel matrices	BNN6 nanoparticles embedded in 3D hydrogel matrices	Light-triggered or chemical diffusion	Localized, sustained NO release for tissue engineering and wound healing	Monotherapy (NO only)	110
BNN6	BTNP-pDA nanoparticles (ultrasound-responsive)	Barium titanate nanoparticles (BTNPs) with polydopamine (pDA); BNN6 surface loading	High-intensity focused ultrasound (HIFU, piezoelectric effect)	>10 fold NO enhancement under HIFU; improved motor coordination and locomotor activity in Parkinson's disease model; neuroprotection of dopaminergic neurons	Monotherapy (NO only)	103

herein were quantified using standard methods such as the Griess assay and chemiluminescence detection, enabling accurate comparison across diverse systems.

2. Engineering of unstable NO donors

Unstable or spontaneous-release NO donors are defined here as basic NO-releasing compounds that readily liberate NO under physiological conditions without the need for enzymatic activation or external stimuli. These donors have been widely used in both fundamental and applied research due to their straightforward synthesis and inherent ability to release NO spontaneously. However, a major limitation of these systems is the difficulty in achieving precise spatial and temporal control over NO release. To address this challenge, recent efforts have focused on preserving the core structures of these donors while integrating them into diverse delivery platforms, including polymers, nanoparticles, micelles, and related systems, in order to fine-tune NO release kinetics and profiles. In the following sections, we highlight the prototypical unstable NO donors, namely *N*-diazeniumdiolates, *S*-nitrosothiols, and SIN-1, while emphasizing their biochemical characteristics, key limitations, and the platform-based engineering strategies developed to overcome these challenges (Fig. 2).

2.1. *N*-Diazeniumdiolates

N-Diazeniumdiolates, also known as NONOates (1-amino-substituted diazen-1-ium-1,2-diolates), are among the most prominent classes of unstable NO donors. They are readily synthesized by reacting secondary amines with NO gas under elevated pressure (typically ~80 psi).[27–30] Under physiological conditions (~37 °C, pH 7.4), *N*-diazeniumdiolates decompose spontaneously and consistently release two molecules of NO per molecule of donor.[22,31–33] Despite the advantages of this rapid and efficient NO generation, it also makes precise control over the timing and rate of NO delivery *in vivo* challenging. As a result, a substantial fraction of NO may dissipate into the bloodstream before reaching the target site. Conversely, excessive local NO concentrations may accumulate and induce unintended cytotoxic effects. Furthermore, *N*-diazeniumdiolates are highly sensitive to moisture and temperature, which severely limits their shelf stability.[21,22,34–36] To mitigate these issues, numerous structurally modified NONOates with tunable reactivity have been developed. For example, PROLI/NO (a proline-based NONOate) exhibits an extremely short half-life on the order of seconds at 37 °C, whereas DETA/NO (a diethylenetriamine-based NONOate) displays a much longer half-life on the order of tens of hours. Other analogues, such as DMAEP/NO (2-(dimethylamino)ethylputreanine-based NONOate), show intermediate half-lives. Together, these derivatives enable a broad range of controlled NO release profiles.[37–40]

Building on these principles, delivery platform-based strategies have been widely employed to better control NO release from *N*-diazeniumdiolates. In one representative approach, polymers were functionalized with multiple NONOate groups and formulated into both hydrogel and nanoparticle systems. For instance, polyethylenimine (PEI) was reacted with high-pressure NO gas to form a PEI-NONOate polymer, which was subsequently crosslinked into hydrogels or incorporated into poly(lactic-*co*-glycolic acid) (PLGA) nanoparticles. Because *N*-diazeniumdiolate decomposition is acid-catalyzed and follows first-order kinetics under physiological conditions, parameters such as the hydrogel crosslink density or the hydrophobicity of the PLGA matrix govern water diffusion and, therefore, control the NO release rate. Using this platform, free PEI-NONOate in solution released ~50% of its NO payload within the first 30 minutes at pH 7.4 and was nearly completely depleted within 12 hours. In contrast, PLGA-PEI-NONOate nanoparticles exhibited sustained NO release over 6 days with no initial burst, extending the release duration by more than an order of magnitude. This marked prolongation of NO release not only minimized acute cytotoxicity *in vitro* but also significantly enhanced biological performance in endothelial cell adhesion, proliferation, and angiogenesis. These results clearly demonstrate that rational polymer design can transform a fast-releasing NONOate into a precisely controllable and biocompatible NO delivery platform.[31] In another strategy, *N*-diazeniumdiolates were encapsulated within liposomes to improve their stability and modulate their release behavior. Small-molecule NO donors such as SPER/NO and DPTA/NO were loaded into liposomes (~265 nm in diameter, composed of dipalmitoylphosphatidylcholine and cholesterol at a 1 : 1 ratio) using a reverse-phase evaporation method. Encapsulation within the alkaline liposomal core substantially prolonged NO release, with the NO release half-life extended by approximately 4- to 7-fold at pH 7.4 compared with free (unencapsulated) donors. This effect is attributed to the basic interior of the liposome, which slows diazeniumdiolate decomposition. In contrast, under acidic conditions (pH 5.4), proton influx into the liposome rapidly accelerates donor breakdown, triggering a swift burst of NO release within the vesicle. This pH-responsive behavior suggests that liposomal

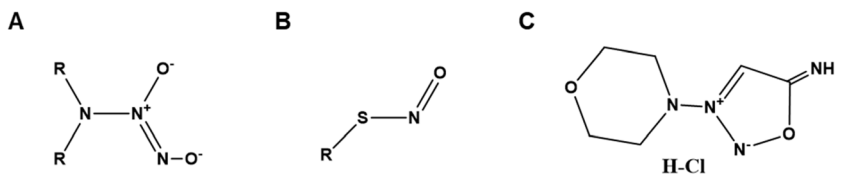

Fig. 2 Chemical structure of unstable NO donors. (A) *N*-Diazeniumdiolates, (B) *S*-nitrosothiols, (C) SIN-1.

carriers can selectively promote NO release in acidic microenvironments, such as the tumor milieu. Consistent with this observation, *in vitro* studies have shown that liposomal DPTA/NO suppresses pancreatic cancer cell (PANC-1) viability at much lower concentrations than the free donor,[41] highlighting the therapeutic advantage of liposomal NO delivery for targeting diseased tissue. Despite the improved control afforded by liposomal vesicles, NO release in these systems is still indirectly influenced by environmental cues such as pH. As a more robust alternative, solid-support platforms have been developed to stably immobilize NO donors and provide finer control over release. One notable example is a sol–gel-derived xerogel system incorporating *N*-diazeniumdiolated silane precursors into a rigid silica-based matrix. Xerogels are porous, dry silica networks formed by sol–gel processing followed by solvent removal. In this approach, various diazeniumdiolate-functionalized alkoxysilanes were co-condensed with phenyltrimethoxysilane (PTMOS) to form NO-releasing xerogels. Entrapment of the NO donor within the rigid siloxane scaffold markedly reduced moisture exposure, thereby greatly enhancing storage stability and improving the reproducibility of NO release. These xerogels achieved high NO loading capacities (1.2 μmol mg^{-1}) and sustained NO release for 20–90 hours under physiological conditions, while also exhibiting minimal silica leaching and low cytotoxicity. Notably, an *N*-diazeniumdiolate-containing xerogel was applied as the outer membrane of glucose biosensors, maintaining high glucose sensitivity (3.4 nA mM^{-1}) for more than 7 days. This result demonstrates the feasibility of xerogel-based platforms for long-term NO release in biomedical devices, offering highly stable and localized NO delivery for applications such as implanted sensors.[42]

2.2. *S*-Nitrosothiol

S-Nitrosothiols (RSNOs) are another important class of unstable NO donors, characterized by an NO group covalently bound to a sulfur atom. Endogenous RSNOs are formed through the *S*-nitrosation of biomolecules' cysteine residues, including glutathione (GSH) and serum albumin.[23,43–45] RSNO compounds are capable of releasing NO under relatively mild physiological conditions, and their release rates can be markedly accelerated by specific stimuli. In particular, exposure to light, transition metal ions (*e.g.*, Cu^{+}, Fe^{2+}), or endogenous reducing agents such as GSH and ascorbic acid can trigger rapid RSNO decomposition and NO liberation.[46–50] While this stimulus-responsive lability can be exploited for on-demand NO delivery, it also renders RSNOs extremely sensitive to environmental factors. In practice, they are highly susceptible to photodegradation and thermal decomposition, making strict temporal control of NO release difficult and severely limiting their storage stability.[49,51–53] Moreover, when administered at high concentrations without appropriate control, RSNO donors may induce cytotoxic effects due to excessive NO generation, posing a risk of unintended tissue damage.[46,54–56]

To overcome these limitations, a variety of structural and materials engineering strategies have been developed. For example, our group previously established NO delivery systems based on *S*-nitrosoglutathione (GSNO), and subsequent studies have further refined this platform. Specifically, a temperature-sensitive hydrogel was fabricated by chemically conjugating Pluronic® F127 with gelatin (F127-*g*-gelatin), enabling sustained NO release from encapsulated GSNO under physiological conditions (37 °C). Notably, we demonstrated that enzymatic degradation by matrix metalloproteinase-9 (MMP-9), which is overexpressed in the tumor microenvironment, could be exploited to further promote localized NO release at tumor sites. This controlled NO release acted synergistically with anti-CTLA-4 antibody (aCTLA-4 mAb)-mediated T cell activation to elicit potent antitumor immune responses.[57] An alternative wound-dressing platform was reported in which GSNO was encapsulated into poly(L-lactic acid) (PLA) microparticles to improve stability and modulate NO release within a hybrid hydrogel-based dressing. Briefly, GSNO was dissolved in water and loaded into PLA microparticles using a water-in-oil-in-water (w/o/w) double-emulsion solvent evaporation method. The resulting particles were then dispersed in a chitosan/β-glycerophosphate temperature-sensitive hydrogel and coated with a decellularized amniotic membrane. The GSNO-loaded microparticles (average diameter ~40.7 μm, encapsulation efficiency ~45.6%) extended the NO release duration by more than two-fold under physiological conditions (37 °C, pH 7.4) compared with free GSNO. The hybrid structure maintained a steady NO release of 24–68 nM per mg over 7 days, effectively suppressing the explosive initial burst observed with free GSNO. Cell viability assays confirmed that the hybrid dressing preserved over 85% viability in human dermal fibroblasts (HDFs), and hemocompatibility tests showed a hemolysis rate below 5%, indicating excellent biocompatibility.[58] Furthermore, a three-dimensional (3D) printing-based NO delivery platform was developed by immobilizing RSNO within a humidity-curable silicone matrix to enhance stability and modulate release. In this approach, RSNOs, including SNAP (*S*-nitroso-*N*-acetylpenicillamine) and GSNO, were admixed with a silicone polymer (Momentive), and NO-releasing silicone tubes were fabricated *via* direct ink writing (DIW) at room temperature. The embedded RSNO crystals (10–50 μm in size) prolonged NO release by approximately 4- to 7-fold (~29 days) under physiological conditions (37 °C) compared to the free donors. This sustained release behavior was attributed to the gradual dissolution of the RSNO crystals within the hydrophobic polymer matrix, enabling continuous NO generation. Notably, incorporating 10 wt% of a low-viscosity polydimethylsiloxane (PDMS; Sylgard 184) led to the spontaneous formation of a drug-free coating layer on the tube surface during printing. This coating reduced the initial NO burst by approximately 21% and smoothed irregular release fluctuations. The 3D-printed RSNO-silicone platform also exhibited reduced bacterial adhesion on rough surfaces and a more stable NO release profile. *In vitro* antimicrobial testing showed that PDMS-coated, SNAP-loaded silicone tubes reduced *Proteus mirabilis* biofilm formation by 66% relative to drug-free controls and by 92% compared with commercial polyurethane catheters.[59] In another study, the NO donor SNAP (*S*-nitroso-*N*-acet-

ylpenicillamine) was encapsulated in a medical-grade CarboSil polymer together with various transition metal nanoparticles (Cu, Fe, Ni, Zn, Ag) to fabricate polymer–metal composite (PMC) structures in both non-layered and layered configurations. SNAP inherently releases NO under physiological conditions (pH 7.4, 37 °C), and the embedded metal nanoparticles catalyze RSNO decomposition, markedly increasing both the release rate and the total NO output. Notably, Cu- and Fe-based composites exhibited a high initial NO flux. In non-layered composites, direct contact between SNAP and the metal nanoparticles induced burst-type NO release, whereas layered composites provided a buffering effect that moderated and prolonged NO release. The overall diffusion rate of SNAP was also substantially higher in non-layered composites, which further accelerated SNAP decomposition. Biocompatibility studies showed that layered composites significantly improved fibroblast viability compared with non-layered counterparts, although SNAP-Zn and SNAP-Cu formulations still exhibited measurable cytotoxicity. In antimicrobial assays, layered SNAP-Cu composites achieved the greatest reduction in methicillin-resistant *Staphylococcus aureus* (MRSA) (~2.13 log reduction), demonstrating a synergistic effect between NO release and the intrinsic antimicrobial activity of copper. Collectively, these findings indicate that metal–polymer layered architectures can maximize NO release while preserving excellent biocompatibility.[60] In another study, an upconversion-ZIF-8 nanocomposite (UCZN) system was developed by growing a porous zeolitic imidazolate framework-8 (ZIF-8) shell on the surface of upconversion nanoparticles (UCNPs) and loading it with *S*-nitrosocysteine (CysNO), an RSNO-type NO donor. This nanoplatform converts tissue-penetrating near-infrared (NIR) light into ultraviolet (UV) emission, which selectively cleaves the S–NO bond in CysNO, thereby enabling spatiotemporally precise, on-demand release of high local concentrations of NO. Unlike free CysNO, which readily decomposes under physiological temperature and pH, the UCZN system minimizes premature NO leakage and exhibits excellent storage stability in the absence of irradiation. However, upon 980 nm laser exposure, it triggers a rapid and robust NO burst with clear on–off switching behavior. In a spinal cord injury (SCI) animal model, this localized NO release attenuated inflammation and reactive gliosis, suppressed neuronal apoptosis, and promoted axonal regeneration, ultimately leading to significant recovery of motor function. This work exemplifies a spatiotemporally controllable NO delivery strategy that overcomes the intrinsic limitations of unstable free donors and maximizes the multifaceted therapeutic potential of NO in treating refractory neurological disorders.[61]

2.3. SIN-1

3-Morpholinosydnonimine (SIN-1) is a prototypical sydnonimine-class NO donor that non-enzymatically generates both NO and the superoxide anion ($O_2^{\bullet-}$) simultaneously under physiological conditions. Its precursor, molsidomine, has been used for decades as a therapeutic agent for the treatment of angina pectoris.[62–69] As SIN-1 undergoes spontaneous decomposition in aqueous solution, the released NO can participate in normal signaling pathways; however, the concurrently generated superoxide readily reacts with NO to form peroxynitrite ($ONOO^-$), a highly reactive species that induces strong oxidative and nitrosative stress.[46,62,70,71] Light exposure (approximately 3500 lux) further accelerates NO release, highlighting the pronounced photosensitivity of SIN-1.[72] Despite its pharmacological relevance, SIN-1 suffers from poor storage stability and rapid decomposition under physiological conditions, which severely limits its utility as a controlled delivery agent. These drawbacks create a substantial risk of unintended premature NO release and excessive peroxynitrite formation, potentially leading to toxic side effects.[62,73,74] To date, relatively few studies have focused on directly modifying the SIN-1 molecule itself to overcome these limitations. Instead, recent efforts have focused on the design of hybrid NO donor systems that exploit the reactivity of SIN-1 by incorporating the sydnonimine moiety into larger, more stable molecular frameworks.

For example, one study demonstrated that *N*-nitrosation of SIN-1 to produce *N*-nitroso-3-morpholinosydnonimine altered its decomposition pathway such that each molecule released up to two equivalents of NO, while simultaneously reducing peroxynitrite generation compared with unmodified SIN-1. This result illustrates that subtle electronic modifications of the sydnonimine scaffold can significantly enhance NO release efficiency while mitigating secondary reactive oxygen species (ROS) production.[75] In another strategy, researchers addressed the rapid decomposition of SIN-1 and excessive ROS generation not by modifying SIN-1 directly, but through a hybrid molecular design. Specifically, a compound termed SA-2 was created by combining a sydnonimine-based NO donor motif with a nitroxide-based antioxidant module and subsequently encapsulating it within poly(lactic-*co*-glycolic acid) (PLGA) nanoparticles. This composite system provided protective effects for endothelial cells and enhanced angiogenic activity at substantially lower concentrations than free SIN-1, while also enabling prolonged NO release and improved storage stability. Through this combined structural and formulation strategy, both the toxicity and instability inherent to SIN-1 were effectively mitigated. Although these approaches have not fully resolved the fundamental limitations of SIN-1, they demonstrate that electronic scaffold modification, hybrid molecular design, and nanoparticle-based delivery can collectively enable more controlled NO release and improved safety for future sydnonimine-class NO donors.[76]

3. Engineering of a stable NO donors

While unstable NO donors offer the advantages of spontaneous NO release and straightforward synthesis, their fundamental limitations, such as unpredictable decomposition kinetics, burst-type release, poor storage stability, and lack of precise spatiotemporal control, which necessitate alternative approaches. To overcome these inherent constraints and

achieve on-demand, stimulus-triggered NO release with enhanced stability and selectivity, a diverse array of stable, stimuli-responsive NO donors has been developed. These systems represent a complementary strategy that builds upon the engineering principles established for unstable donors while introducing new mechanisms for achieving precise control over NO delivery in biological environments. In this section, we examine key classes of stable NO donor platforms, highlighting representative examples, their structural characteristics, and the stimulus-dependent mechanisms governing NO release. Notable examples include O^2-protected diazeniumdiolates (such as JS-K and P-NO), protected SIN-1, nitrobenzene derivatives, and BNN6 (Fig. 3).

3.1. O^2-protected diazeniumdiolate

The O^2-protection strategy was developed to overcome the rapid spontaneous decomposition and premature NO release inherent to unprotected NONOates. This approach involves introducing electron-withdrawing protecting groups at the O^2 position of the NONOate core to suppress decomposition under basal conditions. These protecting groups are selectively removed in response to specific stimuli, including GSH, pH changes, enzymatic activity, and reducing environments. Following deprotection, the original NONOate structure is restored, triggering NO release. This strategy serves a dual purpose: it markedly enhances the storage stability of NONOates while enabling stimulus-dependent, on-demand NO release. Additionally, the hydrophobic nature of many O^2-protecting groups allows the protected NONOates to be stably incorporated into the hydrophobic cores of polymeric delivery vehicles such as micelles and nanoparticles, thereby minimizing unintended NO leakage during circulation. Owing to these advantages, O^2-protection has become a central strategy in drug delivery systems for achieving selective NONOate activation in biological environments. Representative examples, including JS-K and P-NO, are discussed below.

3.1.1. JS-K. JS-K (O^2-(2,4-dinitrophenyl) 1-[(4-ethoxycarbonyl)piperazin-1-yl]diazen-1-ium-1,2-diolate) is a prototypical O^2-protected NONOate bearing a 2,4-dinitrophenyl (DNP) protecting group at the O^2 position. This DNP group enables selective activation under conditions of high cytosolic GSH concentration.[77–82] The protecting group remains stable in normal tissues but is rapidly removed in reducing environments with elevated GSH levels, such as the tumor cell cytoplasm, after which the regenerated NONOate undergoes burst-type NO release.[77,78,83] Owing to this redox-selective activation mechanism, JS-K has been extensively investigated as a redox-triggered NO donor with substantial tumor selectivity.[78,79] However, the hydrophobic DNP moiety renders JS-K extremely poorly soluble in water, making direct administration impractical.[77,84] To address this limitation, JS-K is typically incorporated into hydrophobic-core delivery vehicles, including polymeric micelles, nanoparticles, and liposomes.[35,84,85] These platforms not only improve JS-K solubility and storage stability but also enhance its selective accumulation and activation within target tissues. In addition, delivery systems integrating supplementary stimuli responsiveness, such as pH-sensitive, enzymatic, or additional redox triggers, have further expanded the applicability of O^2-protected NONOate strategies.

For example, a recent study reported a pH- and GSH-dual-responsive nanosystem incorporating JS-K to improve its aqueous solubility and reduce non-selective toxicity. This nanocarrier was designed to gradually disassemble in the mildly acidic tumor microenvironment (pH ≈ 6.5) and subsequently activate JS-K upon exposure to elevated intracellular GSH levels (~10 mM). Notably, this design amplifies the characteristic GSH-dependent removal of JS-K's DNP protecting group and the subsequent activation of the O^2-NONOate at the nanocarrier level. When encapsulated within a hydrophobic nanoparticle core, JS-K remains largely inactive in normal tissues (neutral pH, low GSH). However, within the acidic tumor environment, the nanoparticles destabilize and

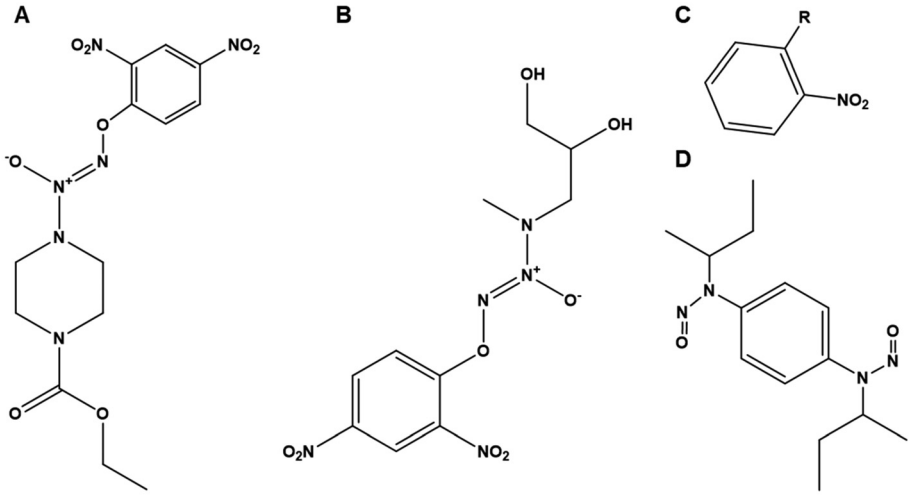

Fig. 3 Chemical structure of stable NO donors. (A) JS-K, (B) P-NO, (C) nitrobenzene, (D) BNN6.

swell; following cellular internalization, GSH-mediated removal of the DNP protecting group triggers a burst-type release of NO. The released NO subsequently reacts with superoxide ($O_2^{\bullet-}$) generated during photodynamic therapy (PDT) to form peroxynitrite, thereby enhancing Type I PDT effects while simultaneously depleting intracellular GSH. This dual action disrupts tumor antioxidant defenses and establishes a synergistic therapeutic mechanism. As a result, the pH/GSH dual-responsive JS-K nanosystem significantly enhanced NO generation and antitumor efficacy compared with free JS-K, while markedly reducing nonspecific activation and systemic toxicity in normal tissues.[86]

In another study, a dimeric JS-K derivative, termed Double JS-K, was incorporated into PEG-based polymeric nanoparticles to modulate JS-K stability and release kinetics through formulation design. Nanoparticles (hundreds of nanometers in diameter) were fabricated from polystyrene-*block*-polyethylene glycol (PS-*b*-PEG) or poly(lactic acid)-*block*-polyethylene glycol (PLA-*b*-PEG) copolymers. Double JS-K was sequestered within the hydrophobic core, creating a steric barrier against the surrounding aqueous environment and GSH. As a result, free Double JS-K in phosphate-buffered saline (PBS; pH 7.4) containing GSH (4 mM) exhibited a very short half-life (~4.5 min), whereas nanoparticle-encapsulated Double JS-K showed an extended half-life of ~40 min, representing more than a ninefold increase in effective NO donor activity duration. This finding demonstrates that combining JS-K-class O^2-protected NONOates with self-assembled nanoparticles provides more than incremental improvements in solubility and physical stability; it substantially prolongs both GSH-triggered activation kinetics and NO release duration.[87] Furthermore, Kaur and colleagues developed a Pluronic P123-based micellar formulation (P123/JS-K) to improve JS-K's poor aqueous solubility and enhance its stability, followed by a detailed investigation of its intracellular distribution. Confocal imaging and cellular fractionation analyses revealed that P123/JS-K micelles exhibited increased cellular uptake and greater accumulation within the cytoplasm and certain organelles compared with free JS-K, indicating that delivery systems can alter intracellular distribution and mechanisms of action.[88] In a subsequent study, the same group systematically evaluated the effects of the Pluronic P123 formulation on the physicochemical properties and anticancer efficacy of JS-K. Compared with free JS-K, P123/JS-K displayed significantly greater stability in PBS, whole blood, plasma, and cell culture media, with markedly slower degradation kinetics. Moreover, the P123 formulation altered the serum protein-binding profile of JS-K, helping to maintain effective drug concentrations *in vivo*. Although P123/JS-K showed anticancer activity in HL-60 and U937 cells comparable to that of free JS-K *in vitro*, it produced substantially greater tumor regression in an HL-60 xenograft NOD/SCID IL2Rγ(null) mouse model. Overall, these findings demonstrate that Pluronic P123 micelles simultaneously enhance the solubility, stability, and pharmacokinetic behavior of JS-K, thereby overcoming key pharmaceutical limitations of O^2-protected diazeniumdiolates through formulation engineering alone, without requiring structural modification.[84]

3.1.2. P-NO. P-NO (O^2-(2,4-dinitrophenyl)-1-[*N*-methyl-(2,3-dihydroxypropyl)amino]-diazenium-1,2-diolate) is an O^2-protected NONOate that incorporates a 2,4-dinitrophenyl (DNP) protecting group at the O^2 position of a diazeniumdiolate bearing a diol moiety. It is structurally designed to achieve both high blood stability and selective intracellular activation.[89] A defining feature of P-NO is its dual responsiveness to GSH and pH. In our previous work, we demonstrated that under endolysosomal conditions (pH 5.0, 50 μM GSH), the DNP protecting group remains largely intact and NO release is minimal. In contrast, rapid deprotection occurs under cytosolic conditions (pH 7.4, 2 mM GSH), triggering a burst-type release of NO. This distinct differential activation forms the core mechanism underlying cytosol-selective NO delivery. Additionally, P-NO selectively associates with phenylboronic acid (PBA)-containing polymer blocks (POEGMA-*b*-PPBA) through its diol moieties to form boronate ester linkages. Through this interaction, P-NO self-assembles into core–shell polymeric micelles (P-NO-PMs). These micelles exhibit excellent blood stability, maintaining structural integrity in the presence of serum proteins (HSA), extracellular GSH (2–20 μM), and high glucose concentrations, with virtually no unintended NO leakage under these conditions. *In vivo*, P-NO-PMs accumulate in tumor tissue through the enhanced permeability and retention (EPR) effect. After cellular internalization, the micelles dissociate in response to endolysosomal pH, releasing P-NO into the cytosol, where the elevated GSH concentration induces deprotection. This process generates a rapid NO burst that produces potent antitumor effects. Overall, P-NO represents a platform-type NO donor based on the O^2-protected diazeniumdiolate strategy, enabling precise coordination of blood stability, cytosol-selective activation, and burst NO release. While it employs the same DNP-based protecting principle as JS-K, P-NO implements a more advanced cytosol-targeted NO delivery strategy by integrating diol-PBA interaction-mediated micellization with dual (pH/GSH) responsiveness (Fig. 4).[89]

3.2. Protected SIN-1

As discussed in section 2.3, the direct use of SIN-1 as an NO delivery agent is severely limited by its rapid decomposition and poor storage stability. To overcome these limitations, several protected SIN-1 strategies have recently been developed, in which SIN-1 is masked as a prodrug or engineered to be regenerated *in situ* only in response to specific stimuli.

For example, a carbohydrate-based targeting approach was designed to overcome the non-specific release and instability of native SIN-1, leading to the development of glycosidase-activated NO donors. In this strategy, SIN-1 was covalently linked to carbohydrates such as glucose, galactose, and *N*-acetylneuraminic acid (sialic acid) *via* glycosyl carbamate linkages, yielding stable prodrug forms (SIN-1-Glucose, SIN-1-Galactose, and SIN-1-NANA). These conjugates significantly enhanced the stability of SIN-1 and were designed to release NO only in the presence of specific glycosidase enzymes. Accordingly, SIN-1-Glucose exhibited approximately 240-fold

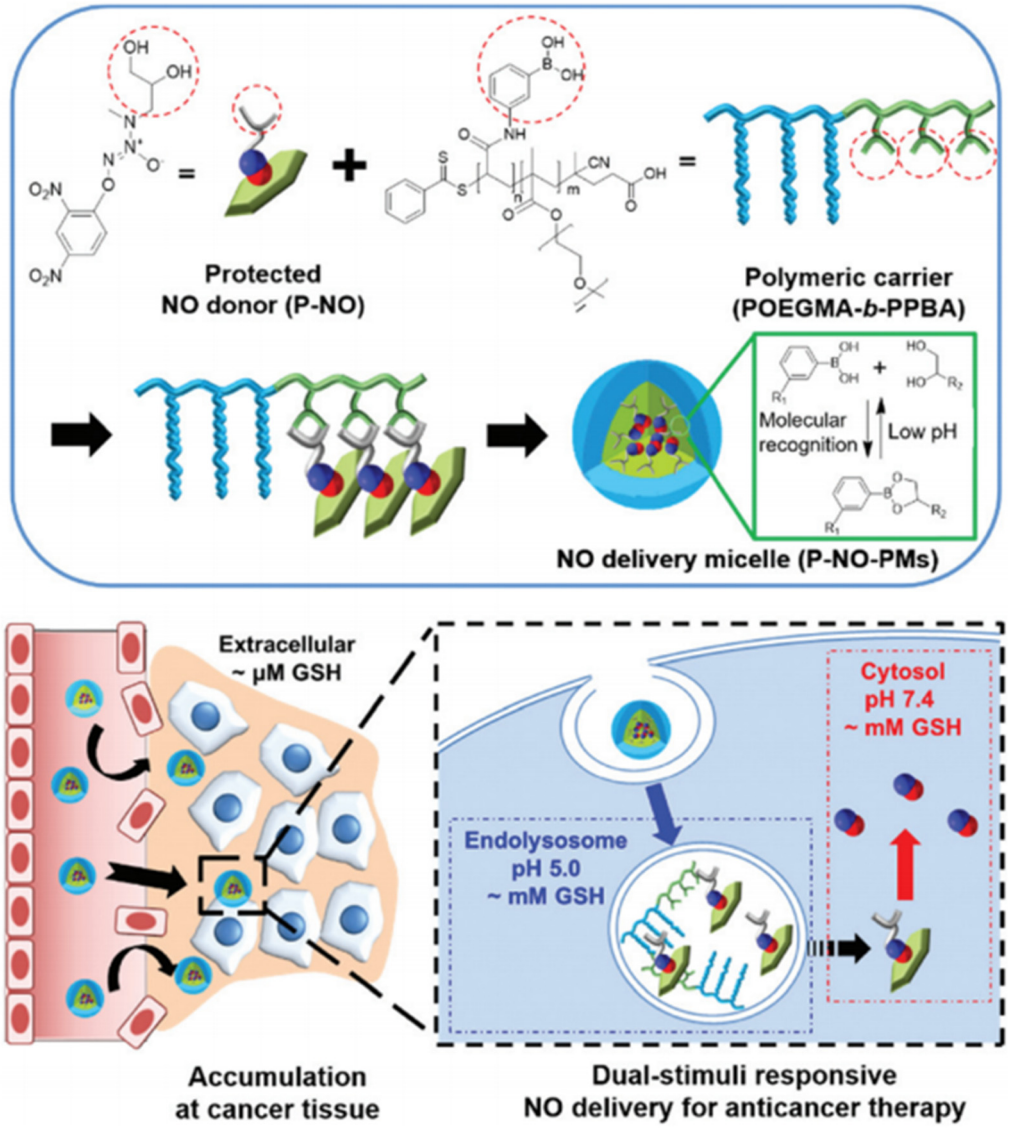

Fig. 4 Schematic illustration of P-NO-PMs-mediated strategy for anticancer treatment. The figure depicts a dual stimuli-responsive polymeric micelle system engineered for cytosol-selective NO delivery. An amphiphilic block copolymer (POEGMA-*b*-PPBA) coordinates with a protected NO donor (P-NO) through phenylboronic acid–diol interaction to form nanoscale micelles that remain stable during blood circulation. Upon tumor cell internalization and exposure to acidic endolysosomal conditions, the boronate ester linkage dissociates, liberating the protected donor into the cytoplasm, where elevated GSH triggers rapid deprotection and burst NO release selectively within cancer cells. Reproduced with permission from ref. 89. Used with permission of Royal Society of Chemistry, from A Cytosol-Selective Nitric Oxide Bomb as a New Paradigm of an Anticancer Drug, *Chem. Commun.*, 2019, **55**(98), 14789–14792; permission conveyed through Copyright Clearance Center, Inc.

higher NO release in the presence of β-glucosidase than in its absence, while SIN-1-Galactose showed an approximately 9.3-fold increase in NO release in the presence of β-galactosidase. These results indicate that such enzyme-responsive conjugates hold promise for biological studies and for applications such as antibody-directed enzyme prodrug therapy (ADEPT).[90] Our group further advanced this concept, developing a self-immolative NO prodrug, SISIN-1, which releases NO under reductive conditions. Briefly, 2,2′-dithiodipyridine was reacted with 2-mercaptoethanol to generate a precursor containing a 2-pyridyl disulfide (PDS) moiety. The hydroxyl group of this precursor was then activated using 4-nitrophenyl chloroformate and subsequently coupled with SIN-1 to form SISIN-1 through a carbamate linkage. This carbamate remains stable under basal conditions. However, in the presence of reducing agents such as GSH or dithiothreitol (DTT), the PDS disulfide bond is cleaved to generate a free thiol. This thiol then undergoes an intramolecular nucleophilic attack to form a five-membered cyclic intermediate, resulting in carbamate cleavage and the release of free SIN-1. Through this self-immolative mechanism, SIN-1 is effectively protected while its NO release is tightly controlled. SISIN-1 is highly stable under physiological

conditions (serum 50 g L^{-1}, cysteine ~50 μM) and under extracellular redox environments ([GSH] = 20 μM). In contrast, it rapidly releases NO at intracellular reductive GSH concentrations ([GSH] = 2 mM), enabling selective NO release in cancer cells, where GSH levels are typically elevated. Moreover, because the PDS moiety is an efficient leaving group, SISIN-1 can undergo thiol-exchange reactions with thiol-containing biomolecules. To further extend its *in vivo* half-life and achieve targeted delivery to lymph nodes, key tissues associated with tumor metastasis, we covalently conjugated SISIN-1 to bovine serum albumin (BSA), generating AL-SISIN-1. AL-SISIN-1 exhibits an average hydrodynamic diameter of approximately 10.6 nm, a size favorable for passive lymphatic drainage and efficient lymph node accumulation. Additionally, it is actively taken up by cancer cells in lymph nodes through interactions with secreted protein acidic and rich in cysteine (SPARC) and gp60 receptors, further enhancing its lymphatic localization. Similar to SISIN-1, AL-SISIN-1 selectively releases NO under reductive conditions, such as the elevated GSH concentrations (~2 mM) present in tumor-metastasized lymph nodes, by activating the self-immolative mechanism of SISIN-1. As a result, AL-SISIN-1 exhibits low systemic toxicity and significant antitumor efficacy in lymph node metastatic cancer models, highlighting its potential as an NO-based targeted therapeutic platform for immune-oncology applications (Fig. 5).[91]

3.3. Nitrobenzene

Nitrobenzene derivatives are photoactivated NO donors that release NO upon light irradiation. Their design typically incorporates bulky *ortho* substituents (*e.g.*, CF_3, methyl, or aryl groups) that twist the nitro moiety, thereby promoting a nitro-to-nitrite photorearrangement pathway.[92–95] This structural feature provides two major advantages: high thermal stability under physiological conditions and precise, light-controlled (on/off) regulation of NO release.

For example, a lipid nanovesicle system (Ves-NTA) was developed by incorporating a 4-nitro-3-(trifluoromethyl)aniline (NTA) derivative into lipid bilayers. In this design, DPPC lipids and the amphiphilic NTA derivative co-assemble into ~100–150 nm vesicles *via* the film hydration method, preserving the twisted nitrobenzene conformation induced by the *ortho*-CF_3 substituent. Upon 410 nm blue-light irradiation, the NTA units within these vesicles undergo nitro-to-nitrite photorearrangement and release NO. The lipid-embedded Ves-NTA system enables NO release in aqueous environments and allows precise tuning of NO output by adjusting the nanovesicle concentration, with fully reversible on/off control by light. Compared with the free NTA derivative in solution, Ves-NTA exhibited slower NO release (half-life ~22.0 to ~38.5 minutes) and maintained higher Neuro-2A cell viability during light irradiation, thereby alleviating the solubility, stability, and cytotoxicity limitations associated with conventional nitrobenzene donors.[96]

A major limitation of classical nitrobenzene donors is their dependence on UV light (315–420 nm) for activation, which can cause phototoxicity in healthy tissues and restrict their clinical applicability.[92,97] Therefore, recent efforts have focused on integrating nitrobenzene motifs into delivery systems to improve light responsiveness and biocompatibility. An important advance addressed the UV activation limitation by shifting the excitation wavelength into the visible range. A mitochondrial-targeted nitrobenzene donor (Rol-DNB-mor/pyr) was developed by conjugating a nitrobenzene moiety with a mitochondrial targeting signal. This compound releases NO upon exposure to 530–590 nm visible light (*e.g.*, 562 nm), effectively overcoming the UV dependence. Electron spin resonance spectroscopy, fluorescence assays, and live-cell imaging verified light-triggered NO generation within mitochondria and demonstrated selective regulation of mitochondrial fission. This strategy partially mitigates the phototoxicity concerns associated with traditional nitrobenzene donors while enabling highly precise control over intracellular NO signaling, with promising potential for mitochondrial-targeted therapeutic applications.[98]

3.4. BNN6

BNN6 (*N*,*N*′-di-*sec*-butyl-*N*,*N*′-dinitroso-1,4-phenylenediamine) is a bis-nitroso, photoresponsive NO donor that releases NO upon UV irradiation, typically at 365 nm. More recently, its activation profile has been expanded to include alternative stimuli, such as ultrasound.[99–103] The bis-nitroso scaffold confers excellent thermal stability under physiological conditions; however, its primary dependence on UV light remains a major limitation for deep-tissue applications and precise *in vivo* NO modulation.[99] To overcome this challenge, a variety of engineering strategies have been developed to integrate BNN6 into diverse material platforms. These designs aim to shift the activation wavelength, most notably into the NIR region, and to enhance spatiotemporal control over NO release through stimulus-responsive on/off regulation.[99,100,103–105] Through these combined molecular and materials-engineering approaches, BNN6 has been progressively developed into a versatile NO donor platform capable of multi-stimuli-responsive and externally controllable therapeutic delivery.

For example, one study reported a NIR-responsive "sandwich" nanomedicine constructed by self-assembling graphene oxide (GO) nanosheets with BNN6 *via* π–π stacking. In the GO-BNN6 construct, hydrophobic BNN6 is intercalated between GO layers, which improves its aqueous dispersibility and stability, while GO absorbs 808 nm NIR light and transfers energy (electrons or heat) to BNN6. As a result, BNN6, which is normally activated only by UV light, can be decomposed under 808 nm irradiation to release NO. The GO-BNN6 hybrid exhibited an exceptionally high loading capacity (~1.2 mg BNN6 per mg GO) and enabled tunable NO release. Both the release rate and total NO output could be precisely controlled by adjusting the NIR power density and irradiation time. In 143B cancer cells, GO-BNN6 functioned as a photo-triggered gas therapeutic, producing NIR on/off-dependent intracellular NO generation and inducing significant cell death.[99]

In another photothermal approach, BNN6 was loaded into polydopamine (pDA)-coated magnetic Fe_3O_4 nanoparticles to

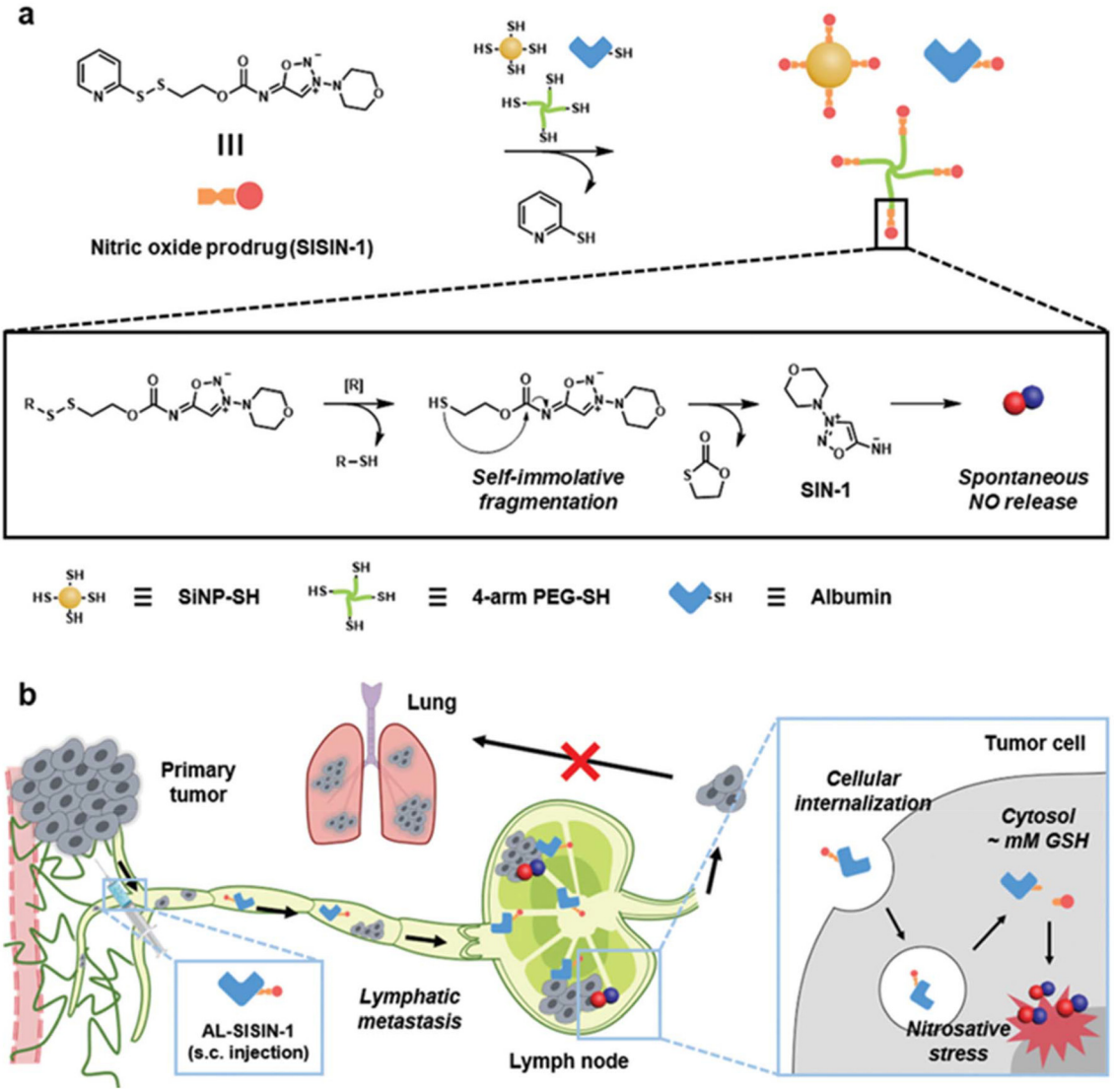

Fig. 5 Schematic illustration of redox-activated SISIN-1 prodrug and lymph node delivery for anti-metastasis. (a) SISIN-1 structure and mechanism: thiol conjugation, reductive disassembly, SIN-1/NO release. [R] = reduction. The self-immolative NO prodrug (SISIN-1) remains stable under extracellular conditions. Upon cellular internalization, elevated GSH cleaves the disulfide bond and triggers intramolecular cyclization, liberating the SIN-1 NO donor. (b) AL-SISIN-1 lymphatic drainage: subcutaneous injection, lymph node accumulation, selective tumor cytotoxicity. Albumin conjugation enables efficient lymphatic drainage to tumor-draining lymph nodes and selective uptake by metastatic cancer cells. Within the intracellular reducing environment, AL-SISIN-1 releases SIN-1 to exert potent tumor-specific cytotoxicity while maintaining excellent systemic safety. Reproduced with permission from ref. 91. Used with permission of John Wiley & Sons, from Lymph-Directed Self-Immolative Nitric Oxide Prodrug for Inhibition of Intractable Metastatic Cancer, *Adv. Sci.*, 2022, **9**(8), 2101935; permission conveyed through Copyright Clearance Center, Inc.

generate an NIR-triggered NO release system. The pDA shell strongly absorbs 808 nm light and generates localized heat, which accelerates the decomposition of the encapsulated BNN6 and promotes NO release. Simultaneously, the Fe_3O_4 magnetic core enables external magnetic targeting. This dual-stimuli (photothermal and magnetic) platform provides finely tunable NO release under NIR on/off control and exhibits potent antibacterial and biofilm-disrupting activity due to the synergistic effects of hyperthermia and NO.[106] Moreover, a two-dimensional bismuth titanate nanosheet ($BiTiS_3$)-BNN6 hybrid has been developed as an on-demand NIR-triggered NO generator. $BiTiS_3$ nanosheets possess strong NIR absorption and excellent photothermal and photoelectronic conversion efficiency. Under 808 nm irradiation, the generated heat and photoelectrons efficiently trigger BNN6 decomposition, resulting in rapid, high-yield NO release. The unique two-dimensional $BiTiS_3$ architecture enhances interfacial electron transfer to BNN6, enabling faster and more efficient NO liberation than that observed with GO-BNN6. This platform achieved robust anti-tumor efficacy *in vivo* under NIR-driven combined NO and photothermal therapy.[107]

The application scope of BNN6 continues to expand. For instance, encapsulation of BNN6 within MOF nanoplatforms, often combined with photothermal agents, enables NIR-trig-

gered combination therapies that integrate photothermal treatment with NO gas therapy.[108] Incorporation of BNN6 into TRPV1-signaling nanocarriers has enabled light-controllable gaseous signaling in neurological disease models.[109] Furthermore, encapsulation of BNN6 nanoparticles within three-dimensional hydrogel matrices provides localized, sustained NO release for tissue engineering and wound healing applications.[110]

More recently, the ultrasound responsiveness of BNN6 has been established as a new modality of stimulus-dependent NO control and has been exploited for the development of high-intensity focused ultrasound (HIFU)-responsive NO delivery systems. The BTNP-pDA-BNN6 system was constructed by coating barium titanate nanoparticles (BTNPs) with pDA, followed by physical loading of BNN6 onto the nanoparticle surface. Upon HIFU irradiation, mechanical deformation induced by the piezoelectric effect activates NO release from BNN6, resulting in more than a 10-fold enhancement in NO generation compared to unexposed controls. In a Parkinson's disease mouse model, systemic nanoparticle administration followed by daily HIFU treatment led to substantial improvements in motor coordination and locomotor activity, accompanied by neuroprotection of dopaminergic neurons and partial restoration of cognitive function.[103]

4. Conclusion

NO-based therapeutics have attracted substantial interest due to the wide-ranging physiological functions and considerable therapeutic potential of NO. However, its gaseous nature, extremely short half-life, and the difficulty of precisely controlling its release in time and space have long constrained its direct clinical application. As reviewed herein, the integration of NO donor molecules with engineered delivery platforms has gained increasing attention as a powerful strategy to overcome these limitations. By combining diverse materials such as polymers, nanocarriers, and stimuli-responsive scaffolds with NO donors, researchers have achieved unprecedented control over NO release kinetics and targeting, greatly expanding the therapeutic feasibility of NO.

Within the spontaneous-release (unstable) donor category, we discussed *N*-diazeniumdiolates, RSNOs, and SIN-1, all of which readily liberate NO under physiological conditions. These donors are easy to synthesize and provide immediate NO release, but they inherently suffer from poor spatiotemporal control. Importantly, recent studies have demonstrated that incorporating these donors into engineered carriers can fundamentally transform their performance. For example, encapsulation of *N*-diazeniumdiolates within PLGA nanoparticles extended NO release duration by more than 12-fold compared with free donors; loading GSNO into MMP-9-degradable hydrogels enabled tumor-selective NO release; and 3D-printed RSNO-based materials markedly enhanced antimicrobial efficacy. Collectively, these examples clearly show that, even without altering donor chemistry, rational platform engineering can dramatically refine NO delivery behavior.

In contrast, the stimuli-responsive (stable) NO donors reviewed herein, including O^2-protected diazeniumdiolates (*e.g.*, JS-K, P-NO), protected SIN-1 prodrugs, nitrobenzene derivatives, and BNN6, remain largely inert until activated by specific triggers. For instance, JS-K and P-NO exploit the elevated GSH levels and acidic pH of tumor microenvironments, while protected SIN-1 prodrugs enable selective cytosolic NO release under reductive conditions. In parallel, nitrobenzene-based donors have progressed from UV-dependent systems to visible- and NIR-responsive platforms, and BNN6 has been hybridized with various nanocomposites to enable efficient NIR photothermal or ultrasound-triggered NO release. Together, these stable donor platforms represent true on-demand NO delivery systems that offer precise external control, thereby improving both therapeutic efficacy and safety.

Overall, a key insight from this review is that NO delivery performance is governed not only by donor molecule design but, critically, by delivery platform engineering. From simple polymer encapsulation to sophisticated nanomaterials responsive to pH, redox conditions, enzymes, light, and even acoustic stimulation, and including hybrid systems incorporating two-dimensional nanomaterials and MOFs, platform design is essential for translating NO therapeutics toward clinical viability. These engineering strategies consistently converge on four core objectives: precise control over the timing, location, and rate of NO release; enhanced storage and *in vivo* stability; minimization of premature NO leakage in non-target tissues; and selective activation at disease sites. Looking forward, research on NO-based drug delivery is expected to progress along several major directions. First, the development of systems responsive to multiple disease-associated cues (*e.g.*, pH, redox status, and enzyme activity) will further enhance selectivity in pathological microenvironments. Second, expanding NIR- and ultrasound-responsive NO donors to overcome the limited tissue penetration of UV and visible light will enable effective NO delivery to deep-seated targets such as solid tumors and chronic infection sites. Third, integrating real-time tracking modalities (*e.g.*, fluorescence, MRI, and PET) into NO delivery platforms will facilitate *in vivo* monitoring of delivery efficiency and therapeutic response. Fourth, advancing co-delivery strategies that combine NO donors with chemotherapeutics, immunomodulators, antioxidants, or other agents within a single platform will enable synergistic therapeutic effects. Finally, greater emphasis on clinical translation, including GMP-compliant manufacturing, comprehensive biocompatibility and safety evaluation, and rational clinical trial design, will be essential for moving NO therapeutics from preclinical proof-of-concept toward clinical practice.

In conclusion, although NO possesses remarkable biological and therapeutic potential, its direct clinical use is intrinsically constrained by its physicochemical properties. The studies reviewed here clearly demonstrate that rational NO donor design, combined with advanced delivery platform

engineering, can systematically overcome these barriers. Ultimately, the successful translation of NO-based therapeutics will depend on close interdisciplinary collaboration across molecular biology, nanotechnology, materials science, and biomedical engineering. With continued progress in novel stimulus-response mechanisms, improved biocompatibility, and regulatory preparedness, NO delivery platforms are well-positioned to become transformative therapeutic modalities for a broad range of applications, including cardiovascular disease, infection control, cancer therapy, and tissue regeneration.

Conflicts of interest

There are no conflicts to declare.

Data availability

No primary research results, software, or code are included in this article, and no new data were generated or analyzed as part of this review.

Acknowledgements

This research was supported by Korea Basic Science Institute (National Research Facilities and Equipment Center) grant funded by the Ministry of Science and ICT (No. RS-2025-00556215) (J. K.). This research was supported by the Chung-Ang University Research Scholarship Grants in 2024 (S.-H. C.).

References

1 R. M. Palmer, A. G. Ferrige and S. Moncada, *Nature*, 1987, **327**, 524–526.
2 J. O. Lundberg and E. Weitzberg, *Cell*, 2022, **185**, 2853–2878.
3 S. Moncada and E. A. Higgs, *Br. J. Pharmacol.*, 2006, **147**(Suppl 1), S193–S201.
4 L. J. Ignarro, G. Cirino, A. Casini and C. Napoli, *J. Cardiovasc. Pharmacol.*, 1999, **34**, 879–886.
5 N. Tuteja, M. Chandra, R. Tuteja and M. K. Misra, *J. Biomed. Biotechnol.*, 2004, **2004**, 227–237.
6 W. Xu, L. Z. Liu, M. Loizidou, M. Ahmed and I. G. Charles, *Cell Res.*, 2002, **12**, 311–320.
7 Z. Wang, A. Jin, Z. Yang and W. Huang, *ACS Nano*, 2023, **17**, 8935–8965.
8 M. R. Miller and I. L. Megson, *Br. J. Pharmacol.*, 2007, **151**, 305–321.
9 M. He, D. Wang, Y. Xu, F. Jiang, J. Zheng, Y. Feng, J. Cao and X. Zhou, *Pharmaceutics*, 2022, **14**, 1345.
10 Y. Li and P. I. Lee, *Mol. Pharm.*, 2010, **7**, 254–266.
11 D. D. Thomas, X. Liu, S. P. Kantrow and J. R. Lancaster Jr., *Proc. Natl. Acad. Sci. U. S. A.*, 2001, **98**, 355–360.
12 M. Kelm, *Biochim. Biophys. Acta*, 1999, **1411**, 273–289.
13 A. J. Gow, B. P. Luchsinger, J. R. Pawloski, D. J. Singel and J. S. Stamler, *Proc. Natl. Acad. Sci. U. S. A.*, 1999, **96**, 9027–9032.
14 J. S. Olson, E. W. Foley, C. Rogge, A. L. Tsai, M. P. Doyle and D. D. Lemon, *Free Radicals Biol. Med.*, 2004, **36**, 685–697.
15 J. Tejero, S. Shiva and M. T. Gladwin, *Physiol. Rev.*, 2019, **99**, 311–379.
16 P. Pacher, J. S. Beckman and L. Liaudet, *Physiol. Rev.*, 2007, **87**, 315–424.
17 B. Weinberger, D. L. Laskin, D. E. Heck and J. D. Laskin, *Toxicol. Sci.*, 2001, **59**, 5–16.
18 V. Krischel, D. Bruch-Gerharz, C. Suschek, K. D. Kröncke, T. Ruzicka and V. Kolb-Bachofen, *J. Invest. Dermatol.*, 1998, **111**, 286–291.
19 L. J. Ignarro, *Proc. Natl. Acad. Sci. U. S. A.*, 2002, **99**, 7816–7817.
20 M. S. França-Silva, C. M. Balarini, J. C. Cruz, B. A. Khan, P. H. Rampelotto and V. A. Braga, *Molecules*, 2014, **19**, 15314–15323.
21 J. Cheng, K. He, Z. Shen, G. Zhang, Y. Yu and J. Hu, *Front. Chem.*, 2019, **7**, 530.
22 L. K. Keefer, *ACS Chem. Biol.*, 2011, **6**, 1147–1155.
23 K. A. Broniowska, A. R. Diers and N. Hogg, *Biochim. Biophys. Acta*, 2013, **1830**, 3173–3181.
24 M. C. Jen, M. C. Serrano, R. van Lith and G. A. Ameer, *Adv. Funct. Mater.*, 2012, **22**, 239–260.
25 C. Q. Li, B. Pang, T. Kiziltepe, L. J. Trudel, B. P. Engelward, P. C. Dedon and G. N. Wogan, *Chem. Res. Toxicol.*, 2006, **19**, 399–406.
26 S. M. Andrabi, N. S. Sharma, A. Karan, S. M. S. Shahriar, B. Cordon, B. Ma and J. Xie, *Adv. Sci.*, 2023, **10**, e2303259.
27 L. K. Keefer, R. W. Nims, K. M. Davies and D. A. Wink, *Methods Enzymol.*, 1996, **268**, 281–293.
28 N. A. Stasko and M. H. Schoenfisch, *J. Am. Chem. Soc.*, 2006, **128**, 8265–8271.
29 J. Konter, G. E. D. A. Abuo-Rahma, A. El-Emam and J. Lehmann, *Eur. J. Org. Chem.*, 2007, 616–624.
30 K. M. Davies, D. A. Wink, J. E. Saavedra and L. K. Keefer, *J. Am. Chem. Soc.*, 2001, **123**, 5473–5481.
31 J. Kim, Y. Lee, K. Singha, H. W. Kim, J. H. Shin, S. Jo, D. K. Han and W. J. Kim, *Bioconjugate Chem.*, 2011, **22**, 1031–1038.
32 Y. Oh, H. Jeong, S. Lim and J. Hong, *Biomacromolecules*, 2020, **21**, 4972–4979.
33 B. Li, Y. Ming, Y. Liu, H. Xing, R. Fu, Z. Li, R. Ni, L. Li, D. Duan, J. Xu, C. Li, M. Xiang, H. Song and J. Chen, *Front. Pharmacol.*, 2020, **11**, 923.
34 J. Kim, G. Saravanakumar, H. W. Choi, D. Park and W. J. Kim, *J. Mater. Chem. B*, 2014, **2**, 341–356.
35 T. Yang, A. N. Zelikin and R. Chandrawati, *Adv. Sci.*, 2018, **5**, 1701043.
36 D. A. Riccio and M. H. Schoenfisch, *Chem. Soc. Rev.*, 2012, **41**, 3731–3741.
37 H. S. Jeh, S. Lu and S. C. George, *J. Microencapsulation*, 2004, **21**, 3–13.

38 S. Waheed, R. Y. Cheng, Y. Casablanca, G. L. Maxwell, D. A. Wink and V. Syed, *Molecules*, 2025, **30**, 4362.
39 J. H. Shin, S. K. Metzger and M. H. Schoenfisch, *J. Am. Chem. Soc.*, 2007, **129**, 4612–4619.
40 J. A. Hrabie and L. K. Keefer, *Chem. Rev.*, 2002, **102**, 1135–1154.
41 D. J. Suchyta and M. H. Schoenfisch, *Mol. Pharm.*, 2015, **12**, 3569–3574.
42 W. L. Storm and M. H. Schoenfisch, *ACS Appl. Mater. Interfaces*, 2013, **5**, 4904–4912.
43 C. E. Paulsen and K. S. Carroll, *Chem. Rev.*, 2013, **113**, 4633–4679.
44 J. S. Stamler, O. Jaraki, J. Osborne, D. I. Simon, J. Keaney, J. Vita, D. Singel, C. R. Valeri and J. Loscalzo, *Proc. Natl. Acad. Sci. U. S. A.*, 1992, **89**, 7674–7677.
45 F. S. Sheu, W. Zhu and P. C. Fung, *Biophys. J.*, 2000, **78**, 1216–1226.
46 J. Kim and S. N. Thomas, *Pharmacol. Rev.*, 2022, **74**, 1146–1175.
47 N. Ryuman, N. Watanabe and T. Arai, *Oxid. Med. Cell. Longevity*, 2011, **2011**, 450317.
48 K. Szaciłowski and Z. Stasicka, *Prog. React. Kinet. Mech.*, 2001, **26**, 1–58.
49 R. J. Singh, N. Hogg, J. Joseph and B. Kalyanaraman, *J. Biol. Chem.*, 1996, **271**, 18596–18603.
50 D. J. Sexton, A. Muruganandam, D. J. McKenney and B. Mutus, *Photochem. Photobiol.*, 1994, **59**, 463–467.
51 M. Ganzarolli de Oliveira, *Basic Clin. Pharmacol. Toxicol.*, 2016, **119**(Suppl 3), 49–56.
52 E. Bechtold and S. B. King, *Antioxid. Redox Signal.*, 2012, **17**, 981–991.
53 M. T. Pelegrino, A. Paganotti, A. B. Seabra and R. B. Weller, *Histochem. Cell Biol.*, 2020, **153**, 431–441.
54 A. Knany, R. Engelman, H. A. Hariri, S. Biswal, H. Wolfenson and M. Benhar, *Free Radicals Biol. Med.*, 2020, **160**, 566–574.
55 A. Jekabsone, Z. Dapkunas, G. C. Brown and V. Borutaite, *Biochem. Pharmacol.*, 2003, **66**, 1513–1519.
56 Y. M. Kim, H. T. Chung, R. L. Simmons and T. R. Billiar, *J. Biol. Chem.*, 2000, **275**, 10954–10961.
57 J. Kim, D. M. Francis, L. F. Sestito, P. A. Archer, M. P. Manspeaker, M. J. O'Melia and S. N. Thomas, *Nat. Commun.*, 2022, **13**, 1479.
58 Z. Bagheri Azizabad, I. Shabani and A. Shabani, *Int. J. Pharm.*, 2025, **668**, 124953.
59 W. Li, Y. Yang, C. J. Ehrhardt, N. Lewinski, D. Gascoyne, G. Lucas, H. Zhao and X. Wang, *ACS Appl. Bio Mater.*, 2021, **4**, 7653–7662.
60 A. Mondal, P. Maffe, S. N. Wilson, S. Ghalei, R. Palacio, H. Handa and E. J. Brisbois, *Mater. Adv.*, 2023, **4**, 3197–3206.
61 Y. Jiang, P. Fu, Y. Liu, C. Wang, P. Zhao, X. Chu, X. Jiang, W. Yang, Y. Wu, Y. Wang, G. Xu, J. Hu and W. Bu, *Sci. Adv.*, 2020, **6**, eabc3513.
62 J. L. Trackey, T. F. Uliasz and S. J. Hewett, *J. Neurochem.*, 2001, **79**, 445–455.
63 P. A. Majid, P. J. DeFeyter, E. E. van der Waals, R. Wardeh and J. P. Roos, *N. Engl. J. Med.*, 1980, **302**, 1–6.
64 N. Hogg, V. M. Darley-Usmar, M. T. Wilson and S. Moncada, *Biochem. J.*, 1992, **281**(Pt 2), 419–424.
65 V. M. Darley-Usmar, N. Hogg, V. J. O'Leary, M. T. Wilson and S. Moncada, *Free Radical Res. Commun.*, 1992, **17**, 9–20.
66 B. Rosenkranz, B. R. Winkelmann and M. J. Parnham, *Clin. Pharmacokinet.*, 1996, **30**, 372–384.
67 M. C. Truss, A. J. Becker, M. H. Djamilian, C. G. Stief and U. Jonas, *Urology*, 1994, **44**, 553–556.
68 H. E. Wegner, H. H. Knispel, T. Meier, R. Klän and K. Miller, *Int. Urol. Nephrol.*, 1995, **27**, 621–628.
69 R. Messin, G. Opolski, T. Fenyvesi, F. Carreer-Bruhwyler, C. Dubois, J. P. Famaey and J. Géczy, *Int. J. Cardiol.*, 2005, **98**, 79–89.
70 R. J. Singh, N. Hogg, J. Joseph, E. Konorev and B. Kalyanaraman, *Arch. Biochem. Biophys.*, 1999, **361**, 331–339.
71 L. M. Landino, B. C. Crews, M. D. Timmons, J. D. Morrow and L. J. Marnett, *Proc. Natl. Acad. Sci. U. S. A.*, 1996, **93**, 15069–15074.
72 T. Ullrich, S. Oberle, A. Abate and H. Schröder, *FEBS Lett.*, 1997, **406**, 66–68.
73 C. Q. Li, L. J. Trudel and G. N. Wogan, *Chem. Res. Toxicol.*, 2002, **15**, 527–535.
74 K. Shirai, T. Okada, K. Konishi, H. Murata, S. Akashi, F. Sugawara, N. Watanabe and T. Arai, *Oxid. Med. Cell. Longevity*, 2012, **2012**, 326731.
75 N. Saffon-Merceron, C. Lherbet and P. Hoffmann, *Molbank*, 2024, **2024**, M1886.
76 D. Q. Le, A. E. Kuriakose, D. X. Nguyen, K. T. Nguyen and S. Acharya, *Sci. Rep.*, 2017, **7**, 8692.
77 H. Chakrapani, R. C. Kalathur, A. E. Maciag, M. L. Citro, X. Ji, L. K. Keefer and J. E. Saavedra, *Bioorg. Med. Chem.*, 2008, **16**, 9764–9771.
78 B. K. Sinha, *J. Cancer Sci. Ther.*, 2016, **8**, 244–251.
79 P. J. Shami, J. E. Saavedra, L. Y. Wang, C. L. Bonifant, B. A. Diwan, S. V. Singh, Y. Gu, S. D. Fox, G. S. Buzard, M. L. Citro, D. J. Waterhouse, K. M. Davies, X. Ji and L. K. Keefer, *Mol. Cancer Ther.*, 2003, **2**, 409–417.
80 A. E. Maciag, H. Chakrapani, J. E. Saavedra, N. L. Morris, R. J. Holland, K. M. Kosak, P. J. Shami, L. M. Anderson and L. K. Keefer, *J. Pharmacol. Exp. Ther.*, 2011, **336**, 313–320.
81 H. Chakrapani, M. M. Goodblatt, V. Udupi, S. Malaviya, P. J. Shami, L. K. Keefer and J. E. Saavedra, *Bioorg. Med. Chem. Lett.*, 2008, **18**, 950–953.
82 P. J. Shami, J. E. Saavedra, C. L. Bonifant, J. Chu, V. Udupi, S. Malaviya, B. I. Carr, S. Kar, M. Wang, L. Jia, X. Ji and L. K. Keefer, *J. Med. Chem.*, 2006, **49**, 4356–4366.
83 L. K. Keefer, *For. Immunopathol. Dis. Ther.*, 2010, **1**, 205–218.
84 I. Kaur, K. M. Kosak, M. Terrazas, J. N. Herron, S. E. Kern, K. M. Boucher and P. J. Shami, *Pharm. Res.*, 2015, **32**, 1395–1406.

85 Y. Liu, X. Wang, J. Li, J. Tang, B. Li, Y. Zhang, N. Gu and F. Yang, *Adv. Mater.*, 2021, **33**, e2101701.
86 J. Zou, Z. Li, Y. Zhu, Y. Tao, Q. You, F. Cao, Q. Wu, M. Wu, J. Cheng, J. Zhu and X. Chen, *Bioact. Mater.*, 2024, **34**, 414–421.
87 V. Kumar, S. Y. Hong, A. E. Maciag, J. E. Saavedra, D. H. Adamson, R. K. Prud'homme, L. K. Keefer and H. Chakrapani, *Mol. Pharm.*, 2010, **7**, 291–298.
88 I. Kaur, M. Terrazas, K. M. Kosak, S. E. Kern, K. M. Boucher and P. J. Shami, *J. Pharm. Pharmacol.*, 2013, **65**, 1329–1336.
89 D. Park, S. Im, G. Saravanakumar, Y. M. Lee, J. Kim, K. Kim, J. Lee, J. Kim and W. J. Kim, *Chem. Commun.*, 2019, **55**, 14789–14792.
90 T. B. Cai, D. Lu, X. Tang, Y. Zhang, M. Landerholm and P. G. Wang, *J. Org. Chem.*, 2005, **70**, 3518–3524.
91 T. Kim, J. Suh, J. Kim and W. J. Kim, *Adv. Sci.*, 2022, **9**, 2101935.
92 T. Suzuki, O. Nagae, Y. Kato, H. Nakagawa, K. Fukuhara and N. Miyata, *J. Am. Chem. Soc.*, 2005, **127**, 11720–11726.
93 L. Saalbach, N. Kotsina, S. W. Crane, M. J. Paterson and D. Townsend, *J. Phys. Chem. A*, 2021, **125**, 7174–7184.
94 A. Giussani and G. A. Worth, *J. Phys. Chem. Lett.*, 2024, **15**, 2216–2221.
95 A. Giussani and G. A. Worth, *Phys. Chem. Chem. Phys.*, 2020, **22**, 15945–15952.
96 N. Sharma, A. K. Dhyani, S. Marepally and D. A. Jose, *Nanoscale Adv.*, 2020, **2**, 463–469.
97 R. Weinstain, T. Slanina, D. Kand and P. Klán, *Chem. Rev.*, 2020, **120**, 13135–13272.
98 K. Kitamura, M. Kawaguchi, N. Ieda, N. Miyata and H. Nakagawa, *ACS Chem. Biol.*, 2016, **11**, 1271–1278.
99 J. Fan, N. He, Q. He, Y. Liu, Y. Ma, X. Fu, Y. Liu, P. Huang and X. Chen, *Nanoscale*, 2015, **7**, 20055–20062.
100 W. Liu, F. Semcheddine, Z. Guo, H. Jiang and X. Wang, *Nanomaterials*, 2022, **12**, 1348.
101 J. Fan, Q. He, Y. Liu, F. Zhang, X. Yang, Z. Wang, N. Lu, W. Fan, L. Lin, G. Niu, N. He, J. Song and X. Chen, *ACS Appl. Mater. Interfaces*, 2016, **8**, 13804–13811.
102 J. Fan, Z. Gao, D. P. Zhao, P. Wang, Z. Z. Wu and X. M. Li, *Med. Gas Res.*, 2019, **9**, 171–175.
103 T. Kim, H. J. Kim, W. Choi, Y. M. Lee, J. H. Pyo, J. Lee, J. Kim, J. Kim, J. H. Kim, C. Kim and W. J. Kim, *Nat. Biomed. Eng.*, 2023, **7**, 149–163.
104 L. Xu, D. Zhang, L. Song, Y. Wu, L. Jiang, Z. Liu, X. Qian, J. Zhou, Y. Liu and Y. Wu, *Mater. Today Bio*, 2025, **34**, 102253.
105 X. Li, Q. Zhang, W. Wu, J. Lin, Y. Liu, L. Chen and X. Qiu, *Biomacromolecules*, 2024, **25**, 6624–6634.
106 X. Yuan, X. Zhao, R. Xia, Z. Xie, Y. Lin and Z. Su, *ACS Appl. Nano Mater.*, 2022, **5**, 18799–18810.
107 M. Jiang, Z. Cheng, T. Luo, C. Chu, Z. Zhang, Y. Hui, P. K. Chu, X. F. Yu, J. Wang, W. Zhou and S. Geng, *Biosens. Bioelectron.*, 2024, **246**, 115895.
108 X. Luo, T. Zhao, S. Qin, F. Wang, J. Ran, Y. Hu and W. Han, *J. Colloid Interface Sci.*, 2025, **684**, 47–59.
109 S. Wang, Y. Wang, J. Lv, C. Xu, Y. Wei, G. Wang and M. Li, *Adv. Healthc. Mater.*, 2024, **13**, e2303579.
110 J. Yang, D. Jia, J. Qiao, X. Peng, C. Zhou and Y. Yang, *Int. J. Nanomed.*, 2024, **19**, 11499–11516.

